Seasonal Patterns of Mpox Index Cases, Africa, 1970–2021

Camille Besombes, Festus Mbrenga, Ella Gonofio, Christian Malaka, Cedric-Stephane Bationo, Jean Gaudart, Manon Curaudeau, Alexandre Hassanin, Antoine Gessain, Romain Duda, Tamara Giles Vernick, Arnaud Fontanet, Emmanuel Nakouné, Jordi Landier

Across 133 confirmed mpox zoonotic index cases reported during 1970–2021 in Africa, cases occurred year-round near the equator, where climate is consistent. However, in tropical regions of the northern hemisphere under a dry/wet season cycle, cases occurred seasonally. Our findings further support the seasonality of mpox zoonotic transmission risk.

Mpox, caused by monkeypox virus (MPXV), remains a neglected tropical zoonotic disease of forested Central and West Africa (*1*). Mpox epidemiology is poorly understood, and the MPXV animal reservoir remains unknown (*1*). Risk factors for zoonotic infection reportedly include direct or indirect contact with wildlife among subsistence activities in forests (*2*–*4*). Those characteristics may have evolved in West Africa because Nigeria reported sustained interhuman transmission of MPXV clade II in 2017, which led to the emergence of clade IIb and the global outbreak declared in May 2022 (*5*). In Central Africa at the time of our study, however, mpox cases remain typically linked to short chains of interhuman transmission after zoonotic spillover (*1*).

After 1990, reported case numbers increased sharply for Congo Basin/clade I, then a sharp increase in West African/clade II began in 2000 (*1*). The lack of systematic surveillance hinders investigative understanding of long-term temporal trends (*1*) and potential seasonality. Available index case time series suggested seasonal changes in risk and high-risk periods: outbreaks occurred predominantly in September in the Central African Republic (CAR) (*6*), and during June–August in different regions of Democratic Republic of the Congo (DRC) (*7*–*11*). We analyzed potential zoonotic transmission seasonality from reported mpox index cases in Africa during 1970–2021.

Author affiliations: Institut Pasteur, Paris, France (C. Besombes, A. Gessain, R. Duda, T. Giles Vernick, A. Fontanet); Institut Pasteur de Bangui, Bangui, Central African Republic (F. Mbrenga, E. Gonofio, C. Malaka, E. Nakouné); Aix Marseille Univ, Marseille, France (C.-S. Bationo, J. Gaudart); Institut de Recherche pour le Développement, Marseille (J. Landier); National Museum of Natural History, Paris (M. Curaudeau, A. Hassanin); Conservatoire National des Arts et métiers, Paris (A. Fontanet)

DOI: http://doi.org/10.3201/eid3005.230293

The Study

We systematically analyzed peer-reviewed and gray literature reporting mpox (formerly monkeypox) index cases from zoonotic origin in Africa during 1970–2021. We extracted index case geographic localization and occurrence dates for temporal and spatial analysis. We used the PubMed query ("1970"[Date-Publication]: "2021/12/31"[Date-Publication]) AND monkeypox AND Africa (Appendix Figure 1, https://wwwnc.cdc.gov/eid/article/30/5/23-0293-App1.pdf).

We only included index cases defined as the first reported case presumed to result from zoonotic transmission in an epidemiologic outbreak investigation. We excluded cases outside Africa and those related to secondary interhuman transmission. We also excluded cases without PCR, viral isolation or culture, or electron microscopy confirmation; and cases without onset month or geographic localization (Appendix Figure 2).

We defined index sites as locations with ≥1 index case. We extracted remotely sensed meteorologic (precipitation, daytime and nighttime temperature), topographic (altitude and slope), land use–land cover data, and fire occurrence data using a 10-km radius buffer zone around each site (Appendix Table 1).

We conducted unsupervised clustering to regroup sites into climate and seasonality (hereafter climate), landscape, and environment profiles. For climate profiles, we included the average

cumulative rainfall, daytime and nighttime temperature, and fire index values (Appendix Table 1) for each month in a principal component analysis. We performed hierarchical clustering on principal components, including 99% of dataset inertia, by using R version 4.3 (The R Foundation for Statistical Computing, https://www.r-project.org) and FactoMineR package (https://cran.r-project.org/web/packages/FactoMineR/index.html). We grouped sites by maximizing within-group similarity and between-groups difference. Following the same approach, we used variables describing the percentage of each buffer occupied by each land use–land cover class (e.g., evergreen closed forest, cropland) and topographic variables to obtain landscape profiles. Finally, we combined the 2 sets of variables to generate combined environment profiles (Appendix).

Table. Location and case characteristics in a study of seasonal patterns of mpox index cases, Africa, 1970–2021

Variable	No. (%) cases, n = 133
Country	
Cameroon	7 (5.3)
Central African Republic	44 (33)
Democratic Republic of the Congo	58 (44)
Gabon	2 (1.5)
Ivory Coast	1 (0.8)
Liberia	5 (3.8)
Nigeria	3 (2.3)
Republic of Congo	8 (6.0)
Sierra Leone	4 (3.0)
South Sudan	1 (0.8)
Timeframe	
1970–1980	35 (26)
1981–1990	8 (6.0)
1991–2000	5 (3.8)
2001–2010	16 (12)
2011–2021	69 (52)
Strain	
Clade I	115 (86)
Clade II	17 (13)
Unknown	1 (0.8)
Outbreak month	
January	15 (11)
February	20 (15)
March	12 (9.0)
April	6 (4.5)
May	7 (5.3)
June	5 (3.8)
July	3 (2.3)
August	14 (11)
September	16 (12)
October	9 (6.8)
November	14 (11)
December	12 (9.0)
Climate or seasonality profile	
Northern hot, wet-dry	23 (17)
Northern cool, wet-dry	47 (35)
Equatorial cool	44 (33)
Southern hot, wet-dry	14 (11)
Other	5 (3.8)
Landscape profile	
Open forest + river or wetlands	23 (17)
Evergreen closed forest	68 (51)
Deciduous forest, closed or open	26 (20)
Grassland + hills	11 (8.3)
Other	5 (3.8)
Combined environmental profile	
Evergreen closed forest + warm night	80 (60)
Evergreen open forest + high precipitation	10 (7.5)
Southern tropical, grassland + hills	14 (11)
Deciduous forest + hot month of January	24 (18)
Other	5 (3.8)

We used the Kruskall-Wallis test to first compare the distribution of latitudes by month of index case occurrence and then to compare months of occurrence according to site environmental characteristics defined by each profile. Using months as a quantitative variable enabled comparison of periods of the year rather than specific months. Sensitivity analyses determined whether the association remained when restricting the analysis to clade II and to recent (2001–2021) cases (Appendix).

We identified 208 index cases: 145 reported from 53 peer-reviewed articles, 26 from 35 gray literature sources, and 37 from CAR national surveillance data (Appendix Figure 2). After exclusion criteria, we retained 133 index cases from 113 sites; 64% were reported from 2000 onward (Appendix Figure 2). Clade I represented 86% of index cases, and clade II represented 13%. DRC accounted for 44% of index cases, and CAR accounted for 33% (Table).

Index cases occurred at a median latitude of 3.44°N (range: −5.87 to 9.53). Index cases latitudes differed significantly across months ($p = 0.0354$). During January–July (April excluded), index cases mostly occurred <3.44°N, whereas during August–December, most cases occurred >3.44°N (Figure 1).

We excluded 4 index sites at high altitude (>1,000 m) and 1 Sahelian index site because rare mpox occurrence prevented seasonality characterization in those settings. The other 108 sites clustered into 4 climate profiles. The equatorial cool profile had temperatures ≤30°C and day-night amplitude ≤10°C, rainfall across all months, and site latitudes ranging from −4.00° to 4.00°N (Figure 2, panels A, B). The northern cool wet-dry profile had similarly low temperatures and amplitude, a dry season during December–February, and site latitudes in the northern hemisphere. The northern hot wet-dry profile displayed temperatures >30°C during the hottest months, a marked dry season during November–March, and latitude sites in the northern hemisphere. The southern hot wet-dry profile had similarly hot temperatures, a dry season in May–August, and latitude sites in the southern hemisphere (Figure 2, panels A, B). Index cases occurred mostly in the equatorial cool (33%),

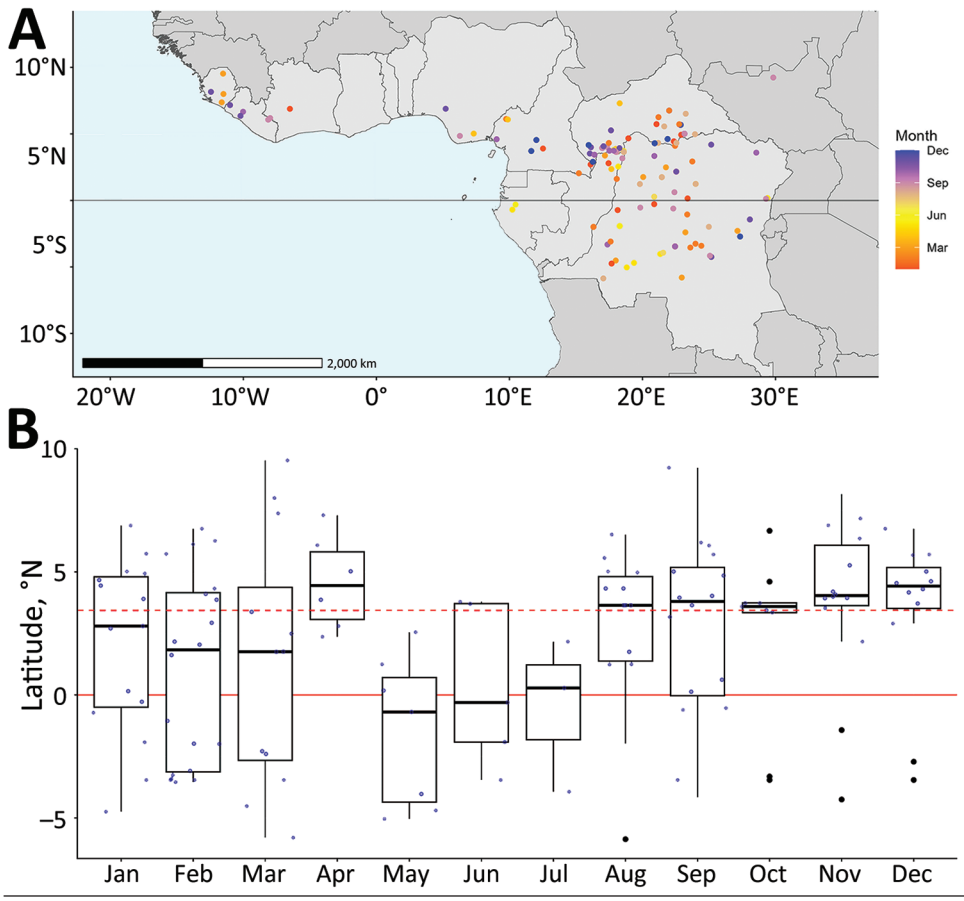

Figure 1. Distribution of cases in study of seasonal patterns of mpox index cases, Africa, 1970–2021. A) Mpox index case sites and month recorded; black horizontal line indicates equator. B) Boxplot of latitude of index case according to month of occurrence. Red dashed line indicates the median latitude of index cases; red solid line indicates the equator (latitude = 0). The thick black line indicates the median latitude, and the box tops and bottom indicate the upper quartile (above) and the lower quartile (below). Whiskers extend from upper quartile to upper quartile+1.5 interquartile range and extend down from lower quartile to lower quartile−1.5 interquartile range. Solid black dots signify outlying observations beyond whiskers range; blue circles identify all other observations.

northern cool wet-dry (35%), and northern hot wet-dry profiles (17%) (Table).

Cases occurred throughout the year in the equatorial cool profile and varied seasonally in the 2 northern wet-dry profiles; cases were nearly absent during April–July (Figure 2, panel C). Seasonality analysis remained inconclusive in the southern hot wet-dry profile, which had low sample size (n = 14). The distribution of index case months was significantly different between climate profiles (p = 0.004). That association persisted in sensitivity analyses (Appendix Tables 2, 3). Landscape and combined environment profiles had poorer association with the month of an index case (Appendix Tables 2, 3, Figures 4, 6, 7).

Conclusions

We showed that the monthly distribution of mpox index cases varied with latitude and was associated with specific climates across the main ecologic mpox niche, excluding high altitude and Sahelian sites. We identified high-risk and low-risk periods across the year in sites located in northern hemisphere climates with alternating dry and wet seasons (>50% of index cases analyzed).

A potential high-risk season occurred during August–March, spanning the last 3 months of the rainy season and all the dry season. That finding suggests complex drivers likely related to human and wildlife ecology. Various seasonal activities can increase human contact with wildlife. During the wet season, human populations settle in forest camps to collect edible caterpillars (*6*), a major source of protein and income (*12*). Hunting and trapping activities, generally conducted year round, intensify during the dry season (*10*). Likewise, dry season slash-and-burn activities tend to drive mammals, notably rodents, toward food resources in neighboring fields, resulting in closer contact with humans.

Multiple obstacles, including access to healthcare, hinder exhaustive mpox reporting from endemic regions. Therefore, this analysis relied on a limited series of well-characterized index cases. Such data and indirect approaches were used extensively to study mpox ecologic niches (*13*) and emerging diseases with similar surveillance gaps (e.g., Ebola virus) (*14*). Our conclusion that MPXV zoonotic transmission risk could be seasonal in regions under a dry-wet season cycle warrants further investigation.

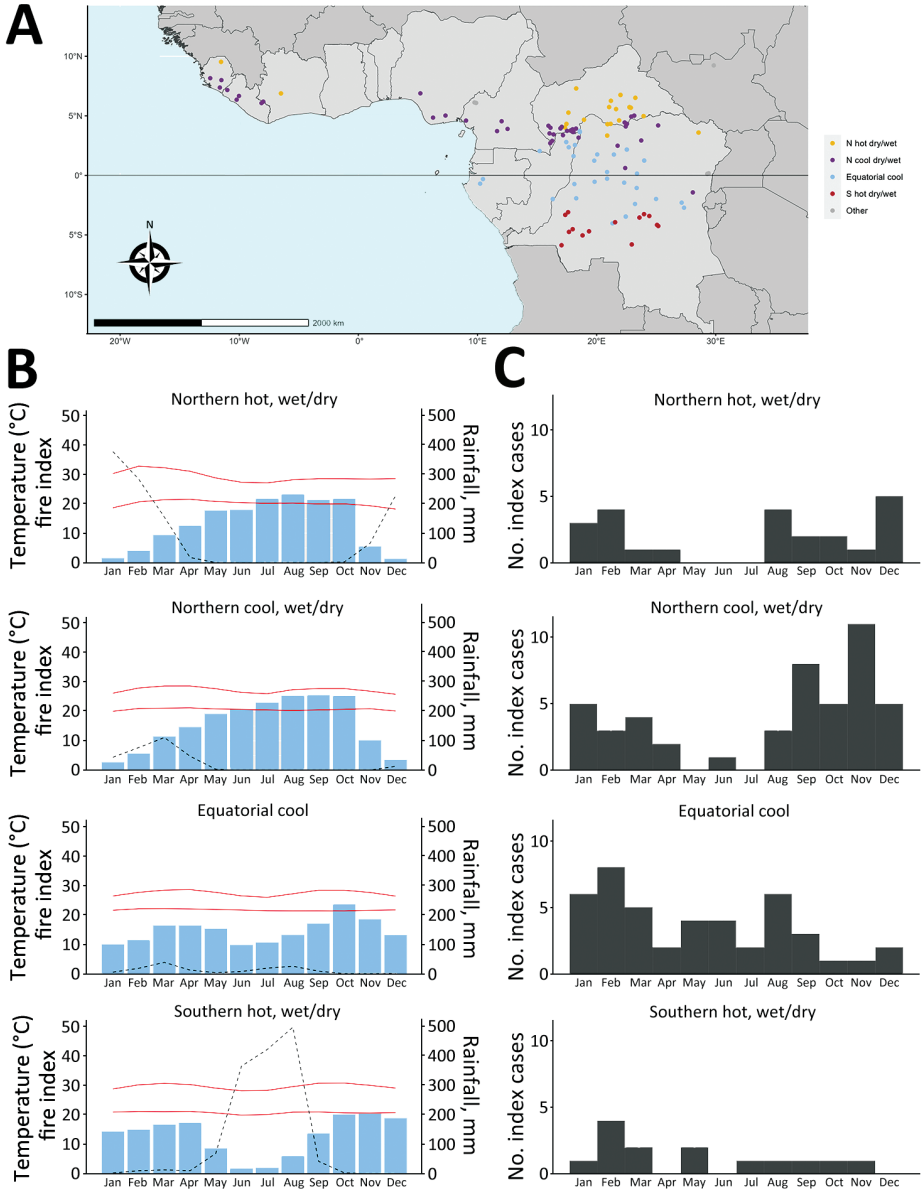

Figure 2. Seasonal distribution of mpox index cases according to the climate profile in Africa, 1970–2021. A) Climate/seasonal profile by site. B) Average monthly rainfall, temperature, and fire index (dotted line) for each climate/seasonal profile. C) Distribution of outbreak index cases by month for each climate/seasonal profile.

Ongoing climate and environmental changes could exacerbate potential underlying seasonal drivers of human MPXV exposure. Determining whether specific seasons or periods bring greater risk for human transmission can improve prevention and surveillance initiatives and contribute to identifying animal reservoirs. For this, a genuine One Health approach is crucial (*15*).

Acknowledgments

Financial support for this study was provided by the French Agence Nationale de Recherche (grant no.: ANR 2019 CE-35), the Projets Transversaux de Recherche (grant no.: PTR 218-19) fund from the Institut Pasteur Paris.

About the Author

Dr. Besombes is an infectious and tropical disease clinician and an epidemiologist, who works as a medical epidemiologist in the Emerging Diseases Epidemiology Unit at Institut Pasteur, Paris, France. Her primary research interests include the understanding of emerging infectious diseases and zoonotic diseases, through One Health and EcoHealth approaches.

References

1. Bunge EM, Hoet B, Chen L, Lienert F, Weidenthaler H, Baer LR, et al. The changing epidemiology of human monkeypox-A potential threat? A systematic review. PLoS Negl Trop Dis. 2022;16:e0010141. https://doi.org/10.1371/journal.pntd.0010141

2. Hutin YJ, Williams RJ, Malfait P, Pebody R, Loparev VN, Ropp SL, et al. Outbreak of human monkeypox, Democratic Republic of Congo, 1996 to 1997. Emerg Infect Dis. 2001;7:434–8. https://doi.org/10.3201/eid0703.017311
3. Patrono LV, Pléh K, Samuni L, Ulrich M, Röthemeier C, Sachse A, et al. Monkeypox virus emergence in wild chimpanzees reveals distinct clinical outcomes and viral diversity. Nat Microbiol. 2020;5:955–65. https://doi.org/10.1038/s41564-020-0706-0
4. Narat V, Alcayna-Stevens L, Rupp S, Giles-Vernick T. Rethinking human-nonhuman primate contact and pathogenic disease spillover. EcoHealth. 2017;14:840–50. https://doi.org/10.1007/s10393-017-1283-4
5. Forni D, Cagliani R, Molteni C, Clerici M, Sironi M. Monkeypox virus: The changing facets of a zoonotic pathogen. Infect Genet Evol. 2022;105:105372. https://doi.org/10.1016/j.meegid.2022.105372
6. Besombes C, Mbrenga F, Schaeffer L, Malaka C, Gonofio E, Landier J, et al. National monkeypox surveillance, Central African Republic, 2001–2021. Emerg Infect Dis. 2022;28:2435–45. https://doi.org/10.3201/eid2812.220897
7. Heymann DL, Szczeniowski M, Esteves K. Re-emergence of monkeypox in Africa: a review of the past six years. Br Med Bull. 1998;54:693–702. https://doi.org/10.1093/oxfordjournals.bmb.a011720
8. Breman JG, Kalisa-Ruti, Steniowski MV, Zanotto E, Gromyko AI, Arita I. Human monkeypox, 1970–79. Bull World Health Organ. 1980;58:165–82.
9. Jezek Z, Grab B, Szczeniowski MV, Paluku KM, Mutombo M. Human monkeypox: secondary attack rates. Bull World Health Organ. 1988;66:465–70.
10. Mandja BM, Brembilla A, Handschumacher P, Bompangue D, Gonzalez JP, Muyembe JJ, et al. Temporal and spatial dynamics of monkeypox in Democratic Republic of Congo, 2000–2015. EcoHealth. 2019;16:476–87. https://doi.org/10.1007/s10393-019-01435-1
11. Ježek Z, Fenner F. Human monkeypox. Basel, Switzerland: S. Karger AG; 1988. https://doi.org/10.1159/isbn.978-3-318-04039-5.
12. Malaisse F, Lognay G. Edible caterpillars from tropical Africa. In: Motte-Florac E, Thomas JMC, eds. "Insects" an oral tradition [in French]. Paris-Louvain: Peeters-SELAF; 2003. pp 279–304.
13. Levine RS, Peterson AT, Yorita KL, Carroll D, Damon IK, Reynolds MG. Ecological niche and geographic distribution of human monkeypox in Africa. PLoS One. 2007;2:e176. https://doi.org/10.1371/journal.pone.0000176
14. Lee-Cruz L, Lenormand M, Cappelle J, Caron A, De Nys H, Peeters M, et al. Mapping of Ebola virus spillover: Suitability and seasonal variability at the landscape scale. PLoS Negl Trop Dis. 2021;15:e0009683. https://doi.org/10.1371/journal.pntd.0009683
15. Mandja BA, Handschumacher P, Bompangue D, Gonzalez JP, Muyembe JJ, Sauleau EA, et al. Environmental drivers of monkeypox transmission in the Democratic Republic of the Congo. EcoHealth. 2022;19:354–64. https://doi.org/10.1007/s10393-022-01610-x

Address for correspondence: Camille Besombes, Institut Pasteur, 211 rue de Vaugirard, Paris 75015, France; email: camille.besombes@sciencespo.fr

Article DOI: http://doi.org/10.3201/eid3005.230293

Seasonal Patterns of Mpox Index Cases, Africa, 1970–2021

Appendix

Mpox Seasonality Analysis

Definition: An index case corresponds to the first reported human case presumed to result from zoonotic transmission after an epidemiologic outbreak investigation.

Systematic Review and Index Case Selection Flowcharts

Sources of gray literature were the Web sites of the World Health Organization (WHO disease outbreak news), the Weekly Bulletin on Outbreaks and other Emergencies, United States Centers for Disease Control and Prevention (CDC), Morbidity and Mortality Weekly Record (MMWR), Africa CDC, Nigeria CDC, ProMed mail and other sources such as Relief web, Outbreak news today or report of outbreak on regional radio confronted to ProMed-mail information (Appendix Figures 1, 2).

Environmental Data Sources

We extracted all environmental data from various open access sources aggregated by the Google Earth Engine platform using the interface provided by R package {rgee} (*1*–*5*). Specifically for Copernicus Global Land Cover dataset, landcover classes retained were: Shrub vegetation (category coded 20), Herbaceous vegetation (code 30), Cropland (code 40), Urban/built-up (code 50), Bare soil (code 60), Waterbodies or wetlands (combining code 80 and 90), Closed forest, evergreen broad leaf (112), Closed forest, deciduous broad leaf (114), Other

closed forest (116), Open forest, evergreen broad leaf (122), Open forest, deciduous broad leaf (124), Other open forest (126) (*5*) (Appendix Table 1).

Environment Profile Generation Methods

We performed multistep nonsupervised analysis (clustering) to classify index case sites according to their environmental features (climate/seasonality, landscape, or combined). The overall method consisted in hierarchical clustering on the principal components of a principal component analysis (PCA) (*6,7*). The first step was a PCA, which is an exploratory method that considers the relationship between variables and reduces complex datasets into fewer dimensions. We performed PCA by using continuous variables. Active variables included:

- For climate/seasonality profile: average monthly cumulative rainfall, daytime temperature, nighttime temperature, fire index from January to December. This profile combine mainly climate-related parameters (temperatures and rainfall), but also fire index which is related to both climate (vegetation has to be dry to burn) but also to human activities (fires are often started by humans, for example to clear and fertilize fields at the start of the planting season).
- For landscape: percentage of surface occupied by Shrub vegetation (category coded 20), Herbaceous vegetation (code 30), Cropland (code 40), Urban/built-up (code 50), Bare soil (code 60), Waterbodies or wetlands (combining code 80 and 90), Closed forest, evergreen broad leaf (112), Closed forest, deciduous broad leaf (114), Other closed forest (116), Open forest, evergreen broad leaf (122), Open forest, deciduous broad leaf (124), Other open forest (126); min, max, mean, median, standard deviation for altitude and slope.
- For combined environment: all variables in the two previous points

To reduce basal noise and ensure a more stable classification, we retained the principal components that summarized 99% of the data. We performed hierarchical ascendant classification on the first 30, 15, and 37 principal components' coordinates, for respectively climate/seasonality, landscape, and combined environment. Each approach provided classes independent of the month of mpox index case occurrence.

Supplementary Results

In addition to climate profiles described in the main article (Appendix Figure 4, panel A), we identified 4 landscape profiles (after excluding the same 5 sites, Appendix Figure 4, panel B). Open forest combined with river or wetland presence (Open+River/wet) occurred mainly in sites bordering the Gulf of Guinea, but also in the Congo Basin. Evergreen closed forest landscape (Evergr. Closed) was dominant in the Congo Basin Forest sites, near the Equator. Deciduous forest landscapes (open or closed) corresponded to inland outbreak sites in the tropical area, at latitudes higher than 5°N or S. Grassland+hill landscape corresponded to sites located around 5°S (Appendix Figures 3, 4).

Regarding the combined environment clustering (landscape+climate, Appendix Figure 4, panel C), profiles combined roughly the climate and landscape profiles and led to one large equatorial profile, regrouping evergreen closed forest with narrow temperature variations and characterized by warmer night temperatures. The clade II/West African outbreak sites were majoritarily in a profile corresponding to evergreen open forest with abundant cumulative precipitation (Ev.open+rain). Sites located around 5°N inland grouped in a deciduous forest group, with hotter temperatures in January (Decid.+hot Ja), while those located around 5°S inland grouped in a grassland+hill profile, both largely similar to the landscapes and climates (Appendix Figure 4, panel A).

Distribution of Mpox Outbreak Months

For all further analyses, we removed the 4 mpox index cases corresponding to the 4 mountains sites (2 in Cameroon and 2 in DRC) located at altitudes >1000m leading to specific climate and topography and 1 index case which occurred in South Sudan, characterized by outlying climate profile (Sahelian) (Appendix Figures 5–7). Combined environmental profile obtained by including climate and landscape data in a single PCA+HCPC.

Sensitivity Analyses on the Association Between Climate/Seasonality Profile and Month of Index Case Occurrence

To test the robustness of the association between climate and month of occurrence of mpox index cases, we conducted several analyses. First, we analyzed all outbreaks across 3 main periods of mpox incidence: 1970–1980 during the smallpox eradication effort; 1981–2000 when outbreaks were only reported in small numbers; and 2001–2021, corresponding to the current context. We then focused specifically on 2001–2021. The main analysis grouped clade I and clade II index cases. There could be differences between the transmission contexts of the two clades, and clade II added a wide geographic area but a limited number of events.

Because our analysis aimed to present hypotheses of current major zoonotic transmission, we studied whether the association identified remained valid for the recent period only (2001–2021) and when considering only clade I cases (which restricted the analysis to central African countries). Since there were only 2 index cases recorded in the Southern hot wet/dry profile over the 2001–2021 period, we also conducted a sensitivity analysis excluding this profile ("After 2000+Clade I, Southern hot wet/dry profile excluded").

We applied these conditions individually or in combination for the 3 profiles defined (climate/seasonality, landscape, and combined environment). The association between climate/seasonality and month of occurrence remained throughout an increasingly homogenous index case sample (Appendix Table 2). For landscapes profile, the association was not significant over the entire set of outbreaks but became significant when excluding events before 2001. This likely led to convergence between landscape and climate/seasonality profiles.

In a second step, we studied whether the bimodal distribution observed in Northern Tropical profiles (cases identified from January to March and from August to December) could have influenced the result of the statistical test. Indeed, in Appendix Figure 8, we presented median and IQR for bimodal distributions in Northern Tropical profiles.

To limit this issue, we defined the start of the mpox epidemiologic year in August, i.e., after minimum occurrence in July (Appendix Figure 9). We replicated the analysis of the distribution of index case month by "epidemiologic year" starting in August, i.e., ending with minimum occurrence in July (Appendix Table 3). This enabled us to account for the fact that

cases in December and January belonged to the same period of the year (i.e., dry season in Northern tropical profiles). We thus confirmed that the difference in distribution identified in Appendix Table 2 was not an artifact related to our analysis using calendar months (Appendix Table 3).

References

1. Funk C, Peterson P, Landsfeld M, Pedreros D, Verdin J, Shukla S, et al. The climate hazards infrared precipitation with stations—a new environmental record for monitoring extremes. Sci Data. 2015;2:150066 PubMed.https://doi.org/10.1038/sdata.2015.66

2. Wan Z, Hook S, Hulley G. 2021. MODIS/Terra Land Surface Temperature/Emissivity Daily L3 Global 1km SIN Grid V061 [Data set]. NASA EOSDros Inf Serv. Land Processes Distributed Active Archive Center. https://doi.org/10.5067/MODIS/MOD11A1.061

3. MODIS/Aqua+Terra Thermal Anomalies/Fire locations 1km V006 and V0061 Standard (Vector data) distributed by LANCE FIRMS https://doi.org/10.5067/FIRMS/MODIS/MCD14ML

4. Farr TG, Rosen PA, Caro E, Crippen R, Duren R, Hensley S, et al. The shuttle radar topography mission. Rev Geophys. 2007;45:RG2004.https://doi.org/10.1029/2005RG000183

5. Buchhorn M, Lesiv M, Tsendbazar N-E, Herold M, Bertels L, Smets, B. Copernicus Global Land Cover Layers-Collection 2. 2020;12(6):1044. https://doi.org/10.3390/rs12061044

6. Lê S, Josse J, Husson F. FactoMineR: an R package for multivariate analysis. J Stat Softw. 2008;25:1–18.https://doi.org/10.18637/jss.v025.i01

7. Griffiths K, Moise K, Piarroux M, Gaudart J, Beaulieu S, Bulit G, et al. Delineating and Analyzing Locality-Level Determinants of Cholera, Haiti. Emerg Infect Dis. 2021;27:170–81. PubMedhttps://doi.org/10.3201/eid2701.191787

Appendix Table 1. Environmental data description

Profile	Data description	Data source	Indicator	N variables	Reference no.
Climate/seasonality	Accumulated precipitation (mm)	CHIRPS	Monthly average, 1981–2021	12	(*1*)
	Daytime average Temperature (°C)	MODIS LST	Monthly average, 2000–2021	12	(*2*)
	Nighttime average Temperature (°C)	MODIS LST	Monthly average, 2000–2021	12	(*2*)
	Fire index (surface burned)	FIRMS	Monthly sum of burned surface 2000–2021	12	(*3*)
Landscape	Altitude (m)	SRTM 30m	Mean, median, min, max, standard deviation	5	(*4*)
	Slope (%)	SRTM 30m	Mean, median, min, max, standard deviation	5	(*4*)
	Land-use-Landcover	Copernicus Global Land Cover	% of Buffer surface in each land-use-landcover class	12	(*5*)
Combined environment	Include all variables from the Climate/Seasonality and Landscape profiles			70	

Appendix Table 2. Results of Kruskall-Wallis test comparing the distribution of index case month of occurrence according to climate/season, landscape and combined environment profile, sorted by calendar year (starting in January). We assessed the robustness of the association in increasingly well characterized and homogenous subsets of data

Conditions	No. index cases included	Climate/ Seasonality	Landscape	Combined environment
All outbreaks	128	0.0042759	0.3364357	0.1751695
Clade I only	112	0.0089514	0.1172652	0.3194001
After 2000 only	81	0.0122368	0.0123876	0.3971197
After 2000+Clade I	73	0.0087610	0.0030186	0.3065604
After 2000+Clade I, Southern hot wet/dry profile excluded	71	0.0060040	0.0044488	0.2895289

Appendix Table 3. Results of Kruskall-wallis test comparing the distribution of mpox index case month of occurrence according to climate/season, landscape and combined environment profile, after ordering the months by mpox epidemiologic year. The red dashed lines indicate the low-risk period in Northern tropical-wet profile. We assessed the robustness of the association in increasingly well characterized and homogenous subsets of data

Conditions	No. index cases included	Climate/ Seasonality	Landscape	Combined environment
All outbreaks	128	0.0047424	0.2001057	0.3011334
Clade I only	112	0.0065628	0.0484065	0.1138376
After 2000 only	81	0.0900866	0.2737394	0.6585237
After 2000+Clade I	73	0.0699108	0.1016864	0.4085023
After 2000+Clade I, Southern hot wet/dry profile excluded	71	0.0453245	0.1288348	0.3711843

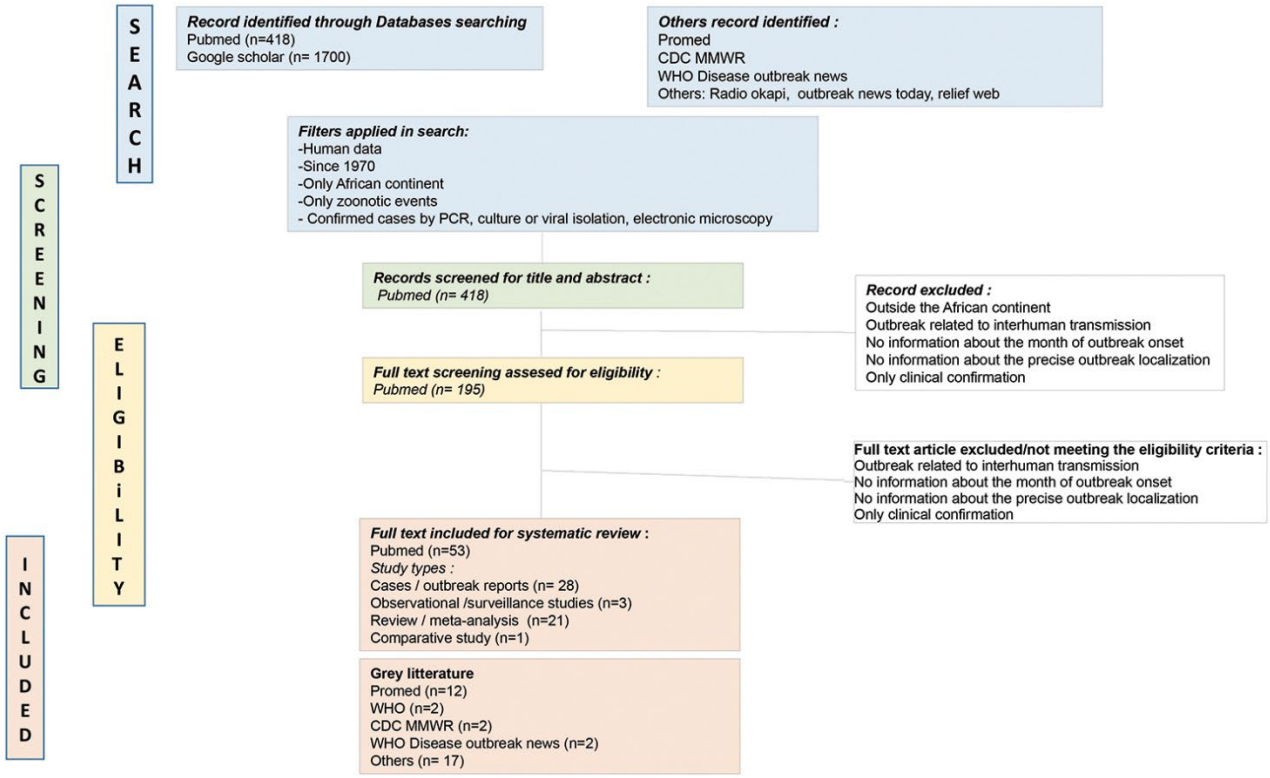

Appendix Figure 1. Systematic review flowchart.

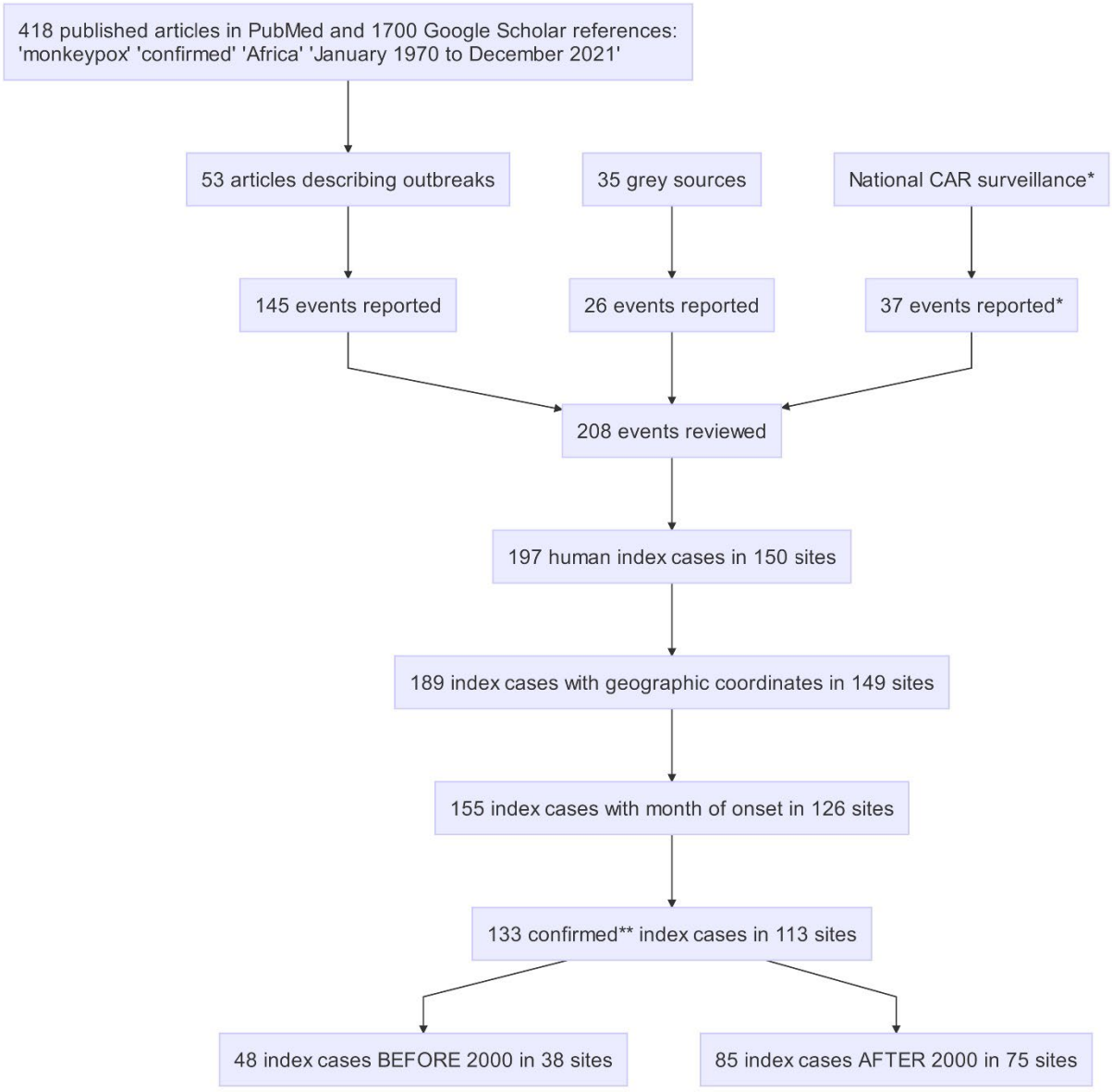

Appendix Figure 2. Detailed flowchart for mpox outbreaks included from the literature review, scientific and gray sources and National Central African Republic (CAR) mpox surveillance provided by the Institut Pasteur de Bangui and the Ministry of Public Health and Population of CAR. *Of 37 unpublished events at the time of review, 26 have been subsequently published by C. Besombes et al., Emerging Infectious Diseases, December 2022 (https://doi.org/10.3201/eid2812.220897). **Confirmation by robust methods only: PCR, viral isolation/culture, or electron microscopy according to inclusion criteria.

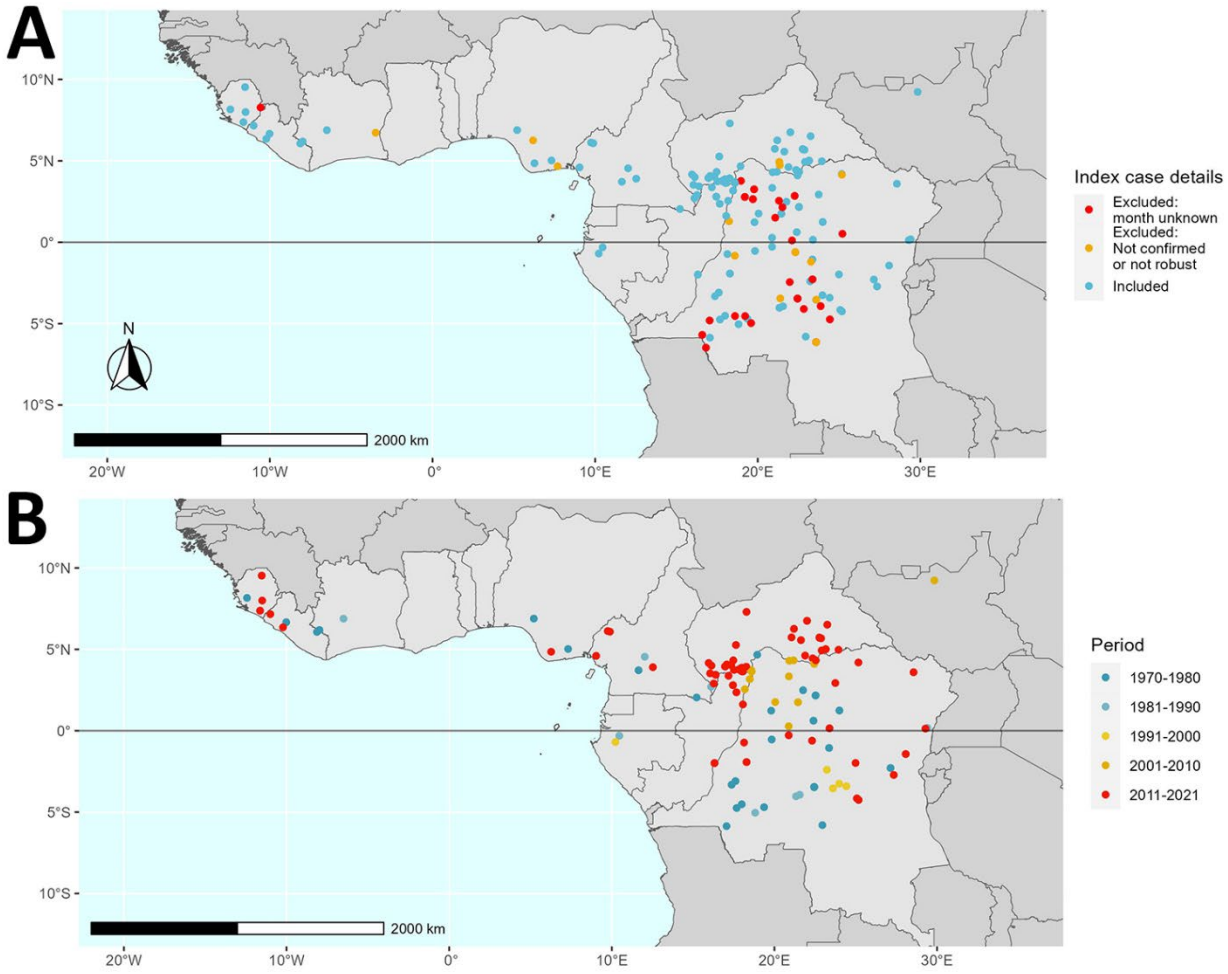

Appendix Figure 3. Map of mpox outbreak sites distribution. A) Human mpox index case sites (n = 149) with geographic coordinates, displaying sites included (blue) or excluded due to unreported month of occurrence (red) or not confirmed by PCR, viral isolation/culture, or electron microscopy (orange). B) Period of outbreak occurrence (n = 113 included sites).

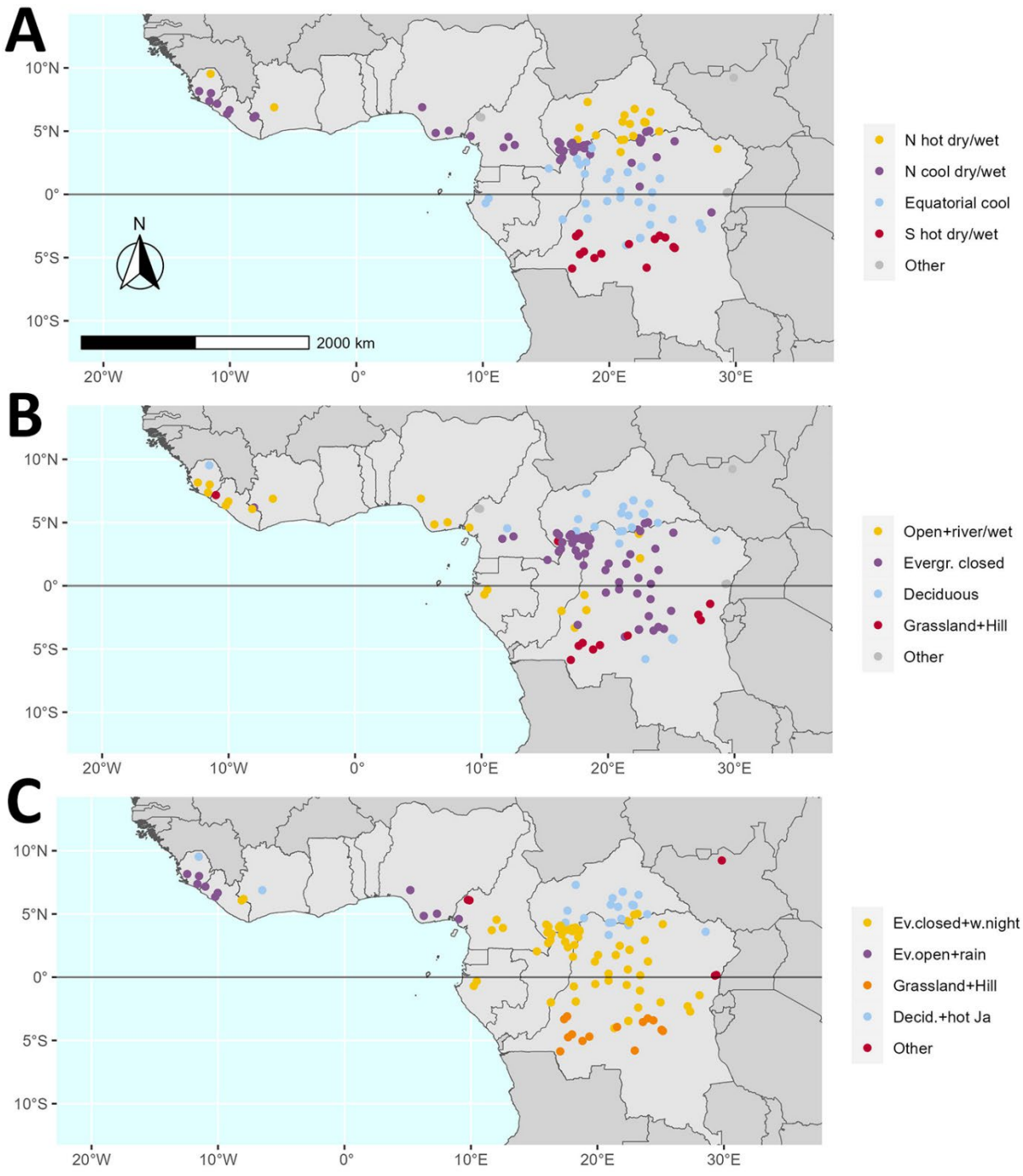

Appendix Figure 4. Maps of mpox outbreak site distributions. A) Climate/seasonality profile. B) Landscape profile. Open+river/wet, open forest + river/wetlands; Evergr. Closed, Evergreen closed forest; Deciduous, deciduous forest; Grassland+Hills; Other, 5 excluded sites. C) Combined seasonal climate and landscape profile. Ev.closed+w.night, evergreen closed forest + warm nights; Ev.open+rain, evergreen open forest + high precipitation volumes; Grassland+Hill, Southern Grassland+Hills; Decid.+hot Ja, deciduous forest + hot month of January; Other, 5 excluded sites.

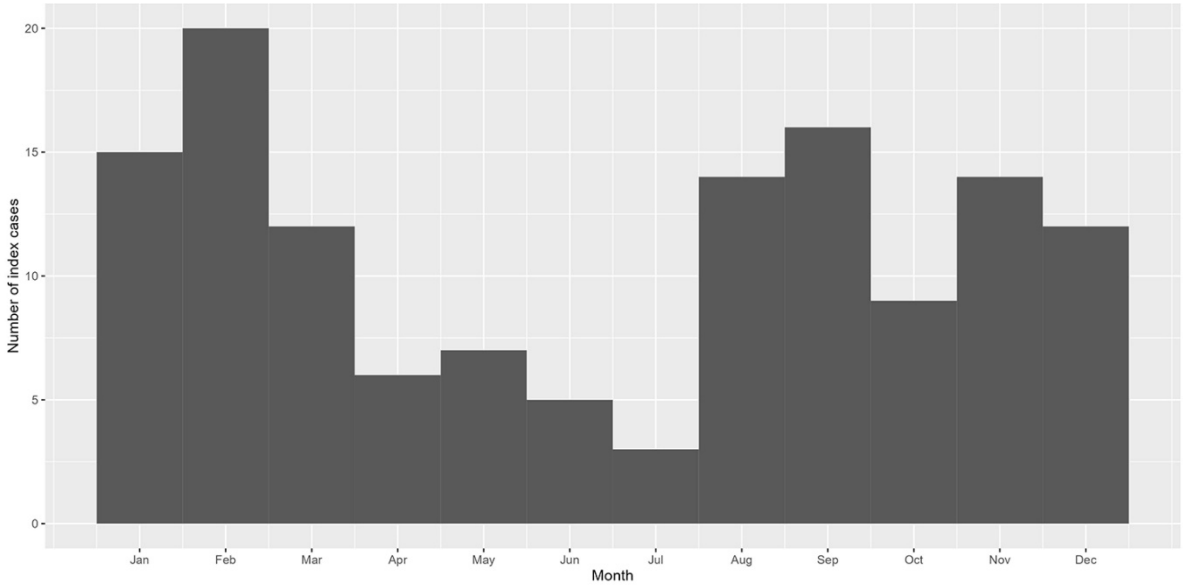

Appendix Figure 5. Distribution of mpox outbreaks by month of occurrence, n = 133 outbreaks.

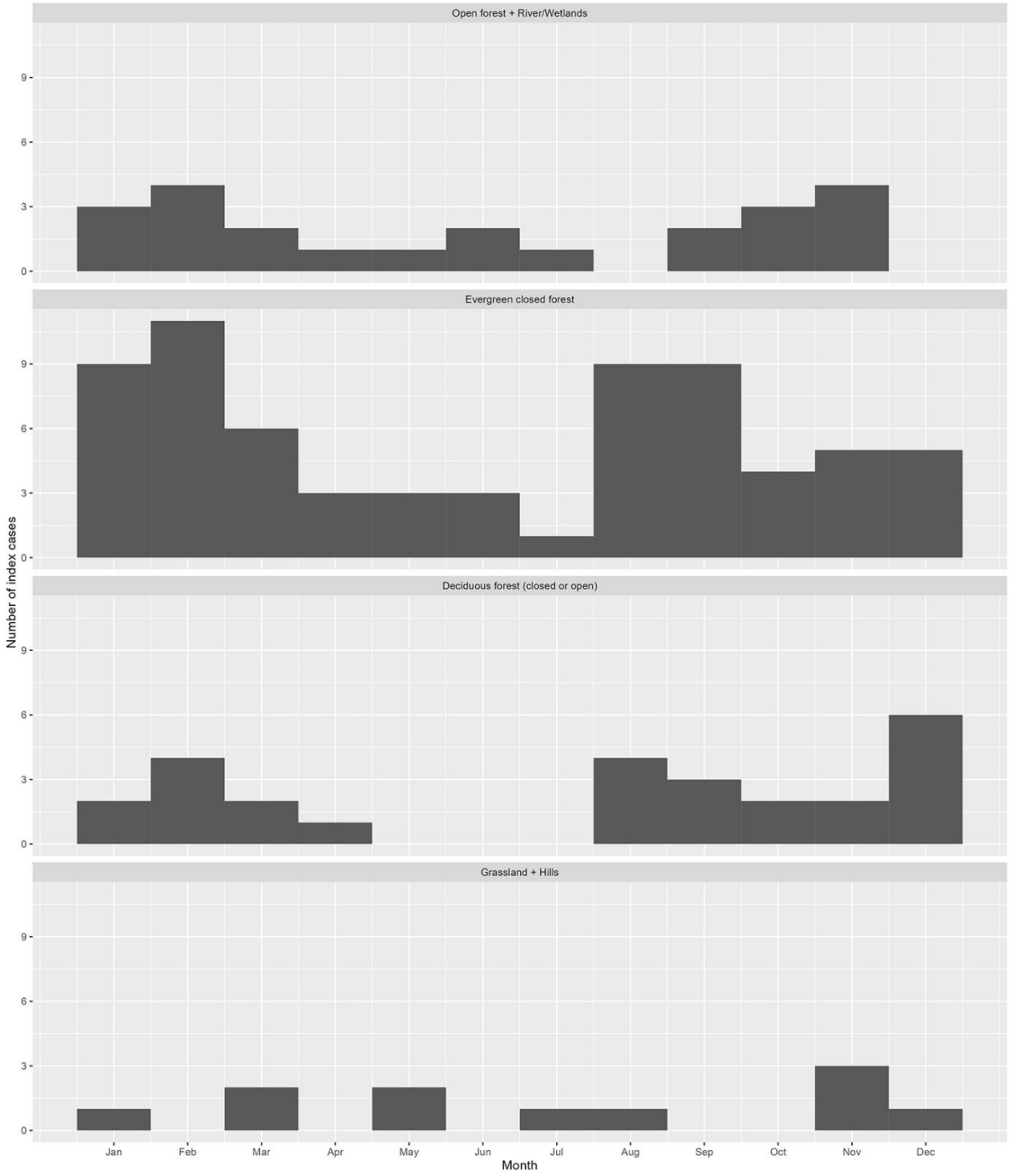

Appendix Figure 6. Distribution of mpox outbreaks by months, according to landscape profile, n = 128 index cases (after excluding 4 high altitude and 1 Sahelian climate locations).

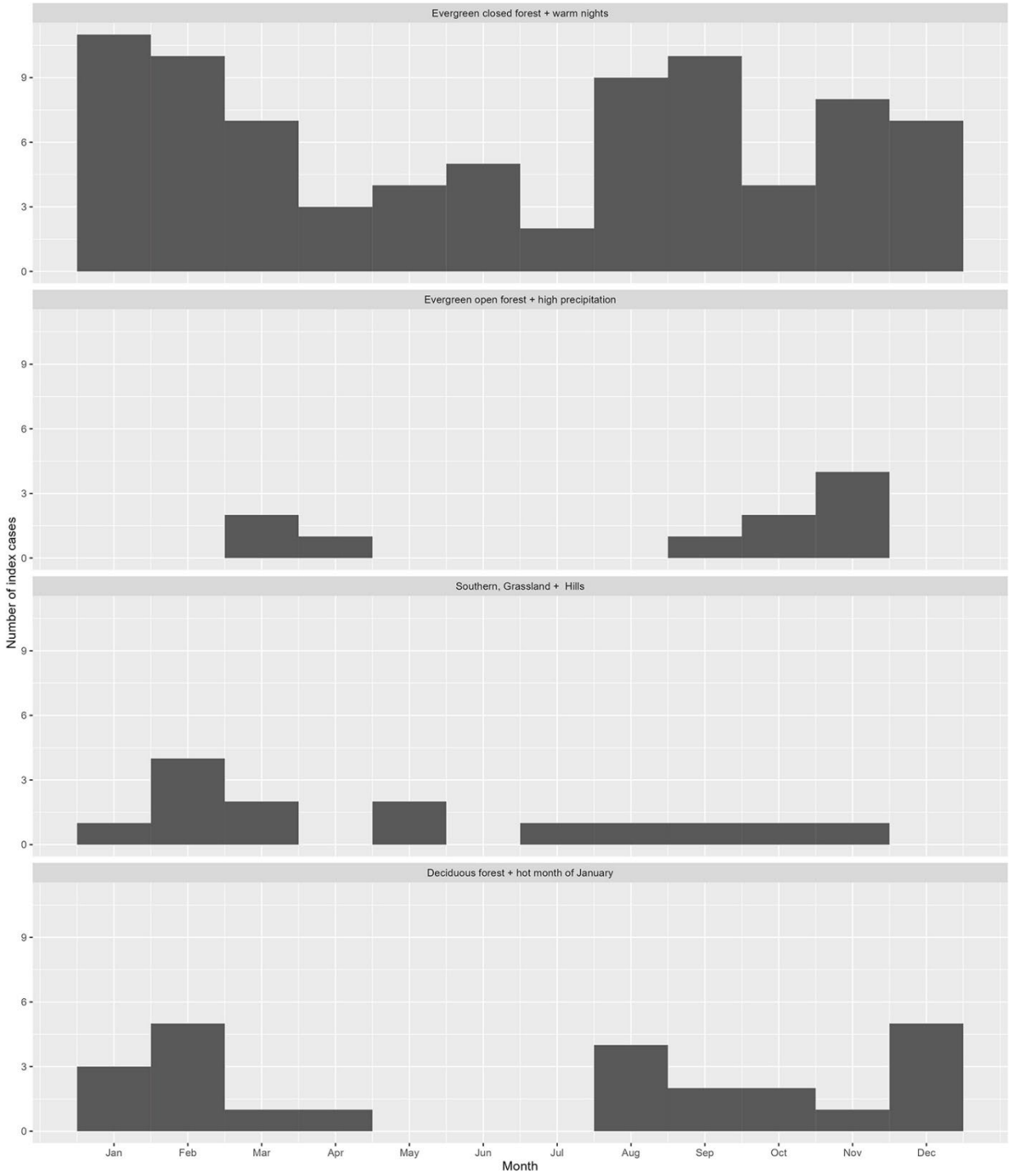

Appendix Figure 7. Distribution of mpox outbreaks by combined profile (landscape and months), n = 128 index cases (after excluding 4 high altitude and 1 Sahelian climate locations).

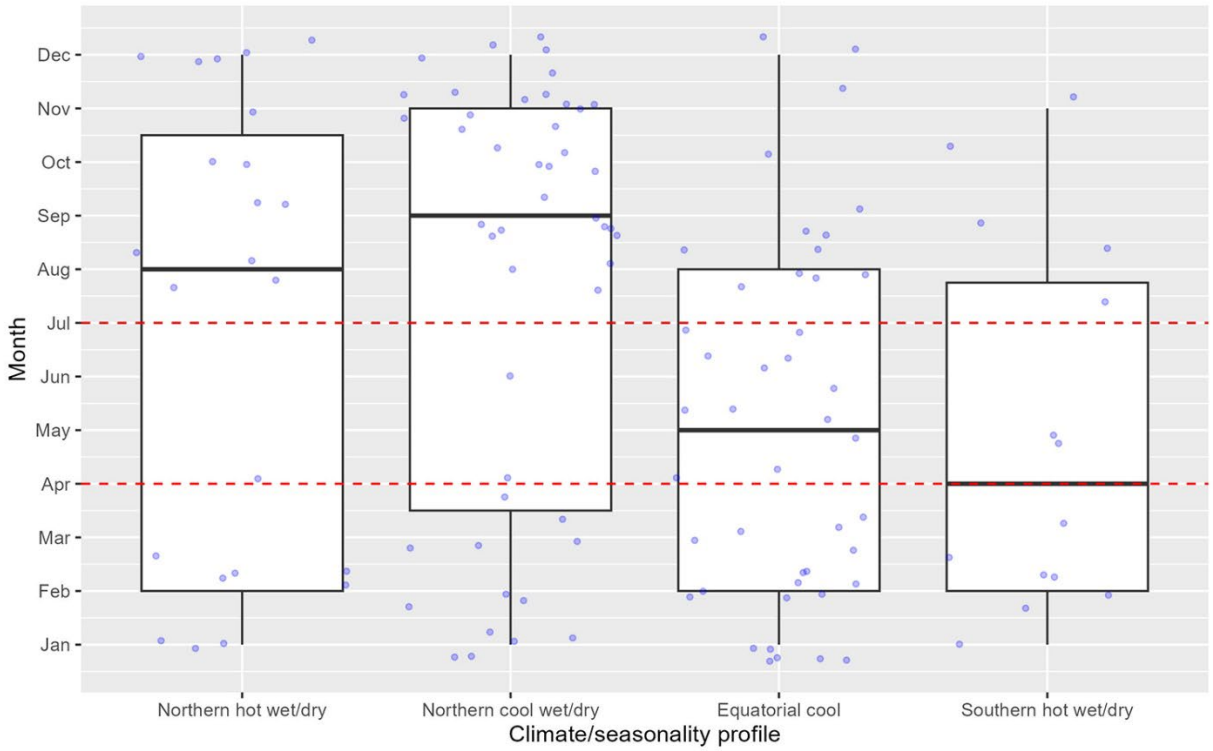

Appendix Figure 8. Boxplot presenting the distribution of months of index case according to the four climate/seasonality profiles. The red dashed lines indicate the low-risk period in the "Northern cool wet/dry" profile, while cases appear well distributed in the "Equatorial cool" profile. Kruskall-Wallis test p-value = 0.0042759 (Appendix Table 2).

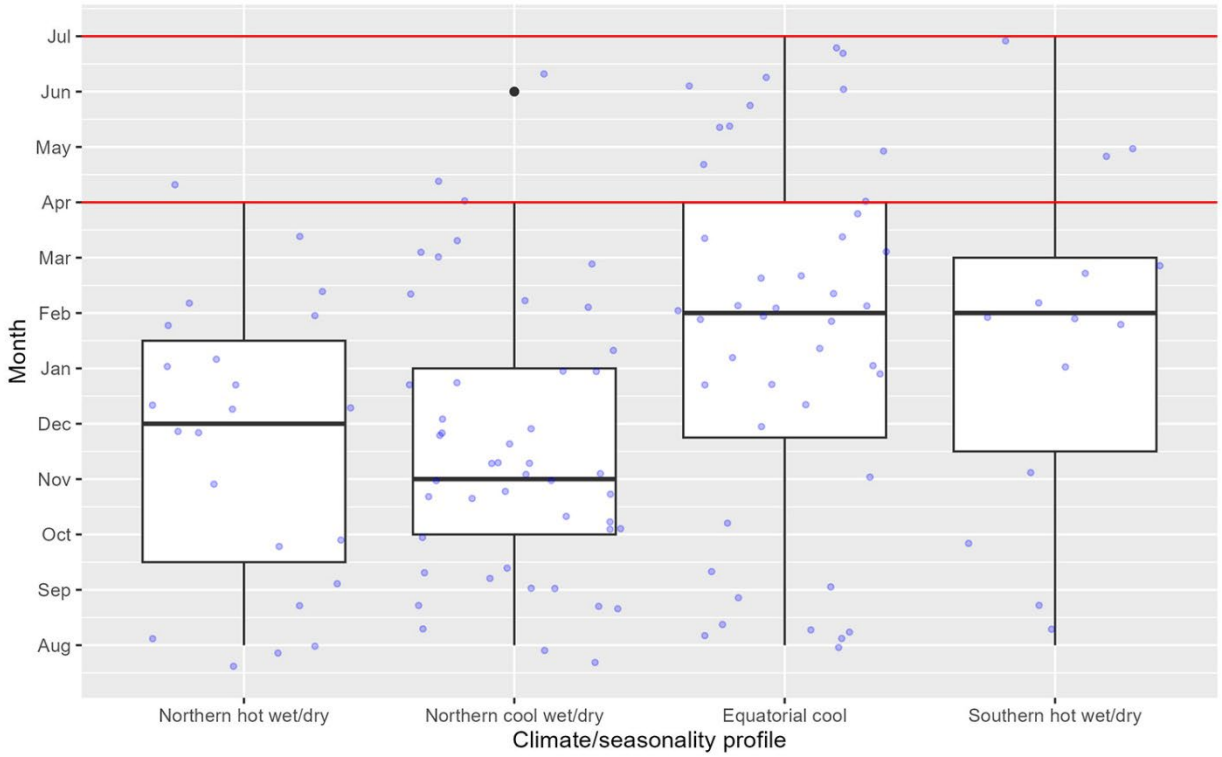

Appendix Figure 9. Boxplot presenting the distribution of months of index case according to the four climate/seasonality profile, starting from the start of the high-risk period and ending at the end of the low-risk period. Kruskall-Wallis test p value = 0.0047 (Appendix Table 3).

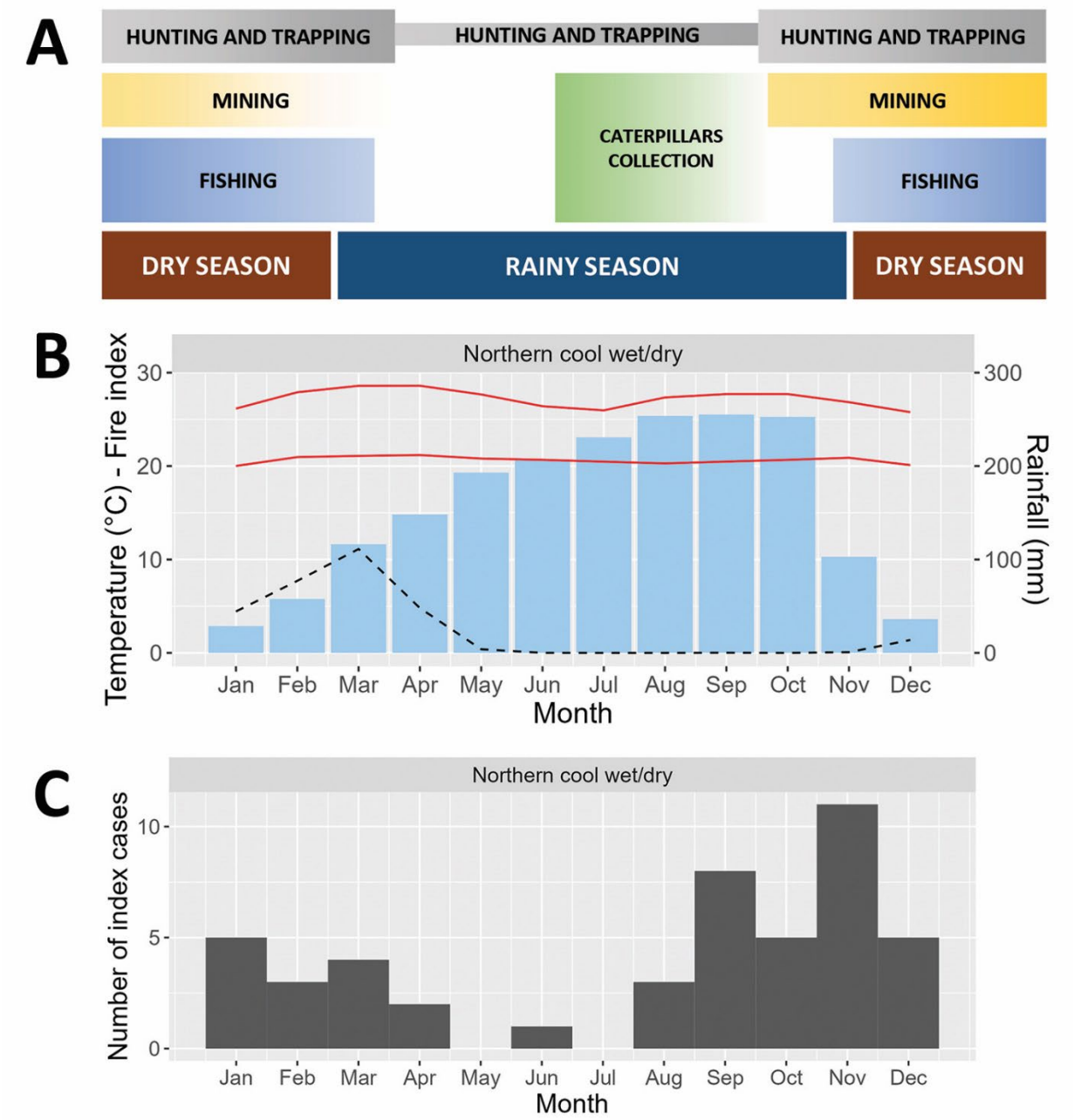

Appendix Figure 10. Schematic representation of possible links between seasonal activities, human exposures (A); climatic variations (B); and mpox zoonotic events (C) in the northern cool wet/dry climate.